



Reconfiguring China's interprovincial rice distribution to support low-carbon goals under climate change

Jintao Yang^{a,b,c}, Fang-He Zhao^c, Manchun Li^d, Penghui Jiang^e, Zhepeng Hu^{b,*}

^a Academy of Global Food Economics and Policy, China Agricultural University, Beijing 100083, China

^b College of Economics and Management, China Agricultural University, Beijing 100083, China

^c State Key Laboratory of Geographic Information Science and Technology, Institute of Geographic Sciences and Natural Resources Research, Chinese Academy of Sciences, Beijing 100101, China

^d School of Geography and Ocean Science, Nanjing University, Nanjing 210023, China

^e School of Public Management, Nanjing Agricultural University, Nanjing 210095, China

ARTICLE INFO

Keywords:

Interprovincial rice trade
Sustainable food distribution
Climate change
Carbon emission

ABSTRACT

Current understanding of low-carbon food distribution is limited by the lack of observed grain flow data and forward-looking scenario analysis. In this study, we construct China's interprovincial rice distribution network for 2020 using 30,524 observed trade records. We then project provincial rice supply and demand dynamics for 2030 under four Shared Socioeconomic Pathway (SSP) scenarios, employing the Global Agro-Ecological Zones (GAEZ) and Future Land Use Simulation (FLUS) models. Subsequently, a scenario-based linear programming framework is applied to explore optimized low-carbon trade configurations. Results indicate that, compared to simulations focused solely on minimizing transport costs, observed trade flows capture substantial long-distance interprovincial exchanges that cost-based models tend to overlook. Moreover, optimized flows could reduce total carbon emissions from rice distribution by 16.1%-20.5% in 2030. These findings offer robust empirical and modeling evidence to inform the reconfiguration of grain distribution systems and support region-specific adaptation strategies under future climate change.

1. Introduction

Rapid urbanization and sustained population growth have intensified both economic and environmental pressures on food supply systems (Deconinck and Toyama, 2022; Karakoc and Konar, 2025). A major structural challenge lies in the spatial mismatch between key agricultural production zones and major urban consumption centers, which are often separated by considerable geographic distances (Xuan et al., 2023). This spatial dislocation not only increases transportation costs but also contributes significantly to greenhouse gas emissions (Liu et al., 2023; Zuo et al., 2023). In addition, the geographic concentration of grain production heightens exposure to climate-induced risks and accelerates environmental degradation in production areas (Chen et al., 2025; Shi et al., 2024). In this context, it is essential to improve our understanding of how climate change interacts with interregional food distribution systems, and to explore strategic reconfigurations of grain distribution that enhance resilience and sustainability.

As food distribution networks expand, accurately capturing

interregional food flows is essential for assessing their embedded environmental impacts (Yang et al., 2025), including carbon emissions, land use, water consumption, and nutrient fluxes (Bai et al., 2024; Chen et al., 2023; Sun et al., 2023; Wu et al., 2018). However, the lack of empirical data on actual interregional food flows has led most studies to rely on simulated flows or proxy-based allocations derived from production-consumption balances and cost-minimizing assumptions (e.g., shortest-path routing) (Croft et al., 2018; Liu et al., 2025). While methodologically convenient, such proxies may overlook the institutional, infrastructural, and climatic complexities that shape real-world logistics (Yang et al., 2021). As a result, estimates of spatially distributed environmental footprints could be distorted, undermining efforts to assign environmental accountability and weakening the design of effective, sustainability-oriented policy interventions.

In addition to data and methodological constraints, the dynamic evolution of agricultural production systems presents further challenges for the accurate characterization of food distribution networks. Land use change has already triggered significant shifts in cropland distribution

* Corresponding author.

E-mail address: zhepenghu@cau.edu.cn (Z. Hu).

<https://doi.org/10.1016/j.resconrec.2026.108816>

Received 29 May 2025; Received in revised form 7 January 2026; Accepted 23 January 2026

Available online 30 January 2026

0921-3449/© 2026 Published by Elsevier B.V.

patterns across various regions (Bosma and Hein, 2023; Bununu et al., 2023; Winkler et al., 2021), while climate change induces regionally differentiated fluctuations in crop yields (Kumar et al., 2022; Liang et al., 2023). These interacting land use and climate dynamics are likely to fundamentally reshape interprovincial grain distribution, introducing substantial uncertainties into the spatial organization of food supply chains (EPA, 2023). To address these challenges, researchers increasingly employed the GAEZ model (Liang et al., 2023; Liao and Wei, 2021), process-based crop models (Gunawat et al., 2022; Yue et al., 2022), and integrated climate scenario pathways (e.g., SSP-RCP) to evaluate the potential impacts of biophysical change on agricultural productivity (M. Li et al., 2023). Given that distribution systems are inherently dependent on the geographic distribution of production, analytical frameworks that fail to incorporate these dynamics risk underestimating the vulnerabilities and adaptive capacities of food systems. Such omissions may constrain the development of effective strategies for decarbonization and climate adaptation in the context of accelerating climate change.

To address these research gaps, this study analyzes China’s interprovincial rice distribution by integrating unique empirical data on actual rice trade flows with scenario-based projections of climate and land-use changes. This integrated approach facilitates a more robust and forward-looking evaluation of carbon-efficient grain supply systems under evolving environmental conditions. Specifically, we aim to: (1) empirically map provincial rice trade flows in 2020 and quantify their associated carbon emissions, thereby overcoming limitations inherent in simulated data; (2) project shifts in provincial rice production patterns by 2030 under various climate and land-use scenarios, and assess how these changes could influence interprovincial rice distribution; and (3) explore optimized strategies to reorganize future rice distribution in ways that minimize consumer-side carbon footprints. By combining observed trade patterns, scenario-based modeling, and optimization methods, our findings provide realistic assessments and practical insights, informing policy efforts to achieve a low-carbon food system in China.

2. Analytical framework and methodology

We propose an integrated three-stage analytical framework to analyze interprovincial rice distribution patterns and carbon footprints in China to identify low-carbon allocations under projected climate and land-use changes: Current State Characterization→Future Projection→Optimization and Reconfiguration (Fig. 1). At the data integration

level, we compile monitoring, predictive, and simulation datasets to construct a comprehensive database capturing rice production-demand balances, trade flows, and carbon emissions across provinces. Methodologically, our framework integrates circulation modeling, carbon footprint accounting, scenario-driven crop yield projections, and optimization techniques aimed at minimizing environmental impacts. The analysis adopts 2020 as the baseline year for current state characterization, as the most recent nationwide monitoring data on empirical interprovincial food trade flows are available for that year. To ensure internal consistency across flow reconstruction, demand estimation, land-use simulation, and yield calibration, all baseline analyses are therefore anchored to 2020. This combined approach facilitates both an accurate depiction of current carbon-embedded rice distribution and robust projections of potential low-carbon allocations amid evolving supply-demand dynamics and emission reduction pressures. The subsequent sections detail the data sources and modeling approaches utilized across these three analytical stages.

2.1. Constructing China’s interprovincial rice distribution network

2.1.1. Empirical mapping of rice trade flows

The interprovincial rice flows in China are primarily driven by three factors: provincial rice production volumes, local consumption demand, and the geographical origins of rice consumed within each province. To empirically characterize these trade patterns, we utilized a comprehensive dataset comprising 30,524 rice samples randomly collected from all 31 provinces, following China’s National Standards for Food Safety Monitoring Sampling as in Yang and Li (2014). The samples were gathered from diverse retail outlets, including farmers’ markets, supermarkets, and specialized grain stores. Each sample documented both the province of sale and the province of rice origin, facilitating an accurate reconstruction of interprovincial rice trade flows. This empirical dataset thus provides a robust foundation for analyzing regional rice sourcing patterns across China.

The volume of rice flowing from province j to province i , denoted as T_{ij} , is calculated using the following expression:

$$T_{ij} = D_i \times p_{ij} \tag{1}$$

where D_i represents the total amount of rice (in tons) imported by province i and p_{ij} indicates the proportion of imported rice in province i that originates from province j based on sampled data. Since D_i can not be directly observed, it is estimated through:

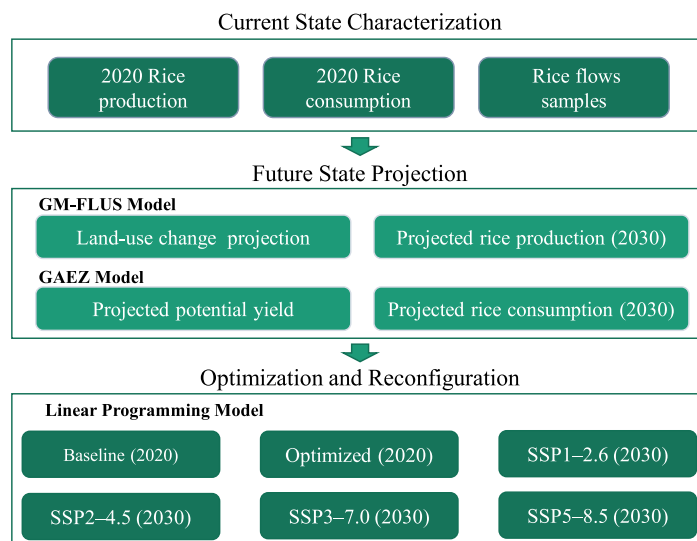


Fig. 1. Integrated framework for low-carbon optimization of China’s interprovincial rice trade.

$$D_i = \sum_k (c_{i,k} \times N_{i,k}) \times 365 - Y_i \quad (2)$$

where Y_i is the total rice production in province i ; $c_{i,k}$ represents the daily per capita rice consumption (kg/person/day) for group k ($k =$ rural or urban) in province i sourced from the China Residents Nutrition and Health Status Monitoring Report (Zhao and He, 2018). For provinces with missing values, estimates were generated using Inverse Distance Weighting (IDW) based on data from neighboring provinces (Figure S1). The variable $N_{i,k}$ is the population size of group k in province i , obtained from the 2020 China Population Census (NBSC, 2021a), while rice production data are sourced from the 2021 China Rural Statistical Yearbook (NBSC, 2021b).

2.1.2. Estimating embedded carbon emissions

Methane (CH₄) and nitrous oxide (N₂O) are the primary greenhouse gases emitted during rice cultivation, jointly accounting for over 85 % of total emissions in this sector (Zhang et al., 2023). Given their substantial interprovincial variation, these two gases are the primary focus of our subsequent linear optimization, enabling a targeted analysis of the most critical emission sources. To quantify the greenhouse gas (GHG) emissions embedded in interprovincial rice flows, this study considers two major sources associated with rice production: (1) CH₄ emissions from paddy field cultivation, and (2) N₂O emissions resulting from the application of nitrogen fertilizers and compound fertilizers. The quantity of greenhouse gas emissions embedded in the flow of rice from province j to province i , denoted as E_{ij} , can be expressed as:

$$E_{ij} = \frac{T_{ij}}{g} \times EF_j \quad (3)$$

where the parameter g represents the milling conversion coefficient from paddy rice to milled rice, set at 0.7 based on existing literature (L. Li et al., 2023) and EF_j denotes the total emission factor associated with rice cultivation in province j , measured in kilograms of CO₂-equivalent per ton and calculated as follows:

$$EF_j = GWP_{CH_4} \cdot E_{CH_4j} / Y_j + GWP_{N_2O} \cdot (E_N \times N_{fertj} + E_F \times F_{fertj}) / Y_j \quad (4)$$

where GWP_{CH_4} and GWP_{N_2O} represent the global warming potentials of methane and nitrous oxide, respectively, set to 27.9 and 273 based on values reported in the IPCC Sixth Assessment Report (IPCC, 2021); Y_j is the total rice production in province j sourced from the 2021 China Rural Statistical Yearbook (NBSC, 2021b); E_{CH_4j} denotes the methane emission factor per unit area for province j , derived from Shen et al. (2024); E_N and E_F represent the emission factors for nitrogen fertilizer and compound fertilizer, respectively, as reported by Min and Hu (2012); and N_{fertj} and F_{fertj} indicate the application rates of nitrogen and compound fertilizer per hectare in province j , based on data from the 2021 China Agricultural Product Cost–Benefit Yearbook (NDRC, 2021).

2.2. Projecting rice production and distribution under 2030 climate scenarios

2.2.1. Land use change forecasting

The GM-FLUS model was employed to simulate future land use in China for the year 2030. It consists of two components: the GM model (Chen and Huang, 2013), which estimates the quantity of land use change, and the FLUS (Future Land Use Simulation) model, which determines spatial distribution patterns. The GM model is based on grey system theory and is particularly suitable for forecasting in systems with limited or uncertain information. The GM model was calibrated using 1 km-resolution remote sensing data collected at five-year intervals from 1990 to 2020, sourced from the Resource and Environmental Science Data Platform of China (<https://www.resdc.cn/>). By analyzing the evolution of land use quantities over time, the model extrapolates future trends and predicts the total area change for each land use type between

2020 and 2030. These projected quantities for 2030 serve as input constraints for the FLUS model, which simulates the spatial configuration of land use types (Figure S2).

The FLUS model is a widely used tool for projecting future land-use types (Liu et al., 2017). It operates under the assumption that whether a specific land parcel will undergo land-use change depends on a combination of environmental conditions (e.g., topography and climate), socio-economic attributes (e.g., population density, GDP), and spatial neighborhood effects. The model learns the relationship between these driving factors and land-use transitions from historical land-use change samples using a data-driven suitability modeling approach, typically based on artificial neural networks. Ten driving factors were selected from three categories: natural conditions, spatial accessibility, and socio-economic attributes. These include elevation, aspect, slope, distance to city center, distance to town center, distance to highways, distance to main roads, distance to railways, GDP, and population. Elevation data were obtained from the Shuttle Radar Topography Mission, from which slope and aspect were derived. Spatial accessibility data were sourced from OpenStreetMap, while GDP and population statistics were provided by the China National Bureau of Statistics (NBSC, 2023). The artificial neural network (ANN) embedded in the FLUS model was configured in random sampling mode, with the following parameter settings: sampling size of 20, 12 hidden layers, 300 iterations, a neighborhood size (N) of 3, and an inertia (acceleration) factor of 0.1.

2.2.2. Projecting rice yield under future climate scenarios

To simulate potential rice yields in 2030, we employed the Global Agro-Ecological Zones (GAEZ) model developed by the Food and Agriculture Organization (FAO) and the International Institute for Applied Systems Analysis (IIASA) (FAO and IIASA, 2021). The GAEZ model estimates attainable crop yields under specified input and management assumptions by integrating key agroclimatic variables such as temperature, precipitation, and solar radiation that affect thermal and moisture suitability, crop phenology, and photosynthetic potential. To reflect a wide range of plausible future climate conditions, we incorporated four combined Shared Socioeconomic Pathway-Representative Concentration Pathway (SSP-RCP) scenarios as inputs: SSP1–2.6, SSP2–4.5, SSP3–7.0, and SSP5–8.5. The Shared Socioeconomic Pathways (SSPs) framework was developed by the Intergovernmental Panel on Climate Change (IPCC) in its Sixth Assessment Report (AR6) and coordinated under the Scenario MIP project. Specifically, SSP1–2.6 represents a sustainable development pathway with strong international cooperation, early emissions peaking, and a projected global warming of approximately 1.8 °C by 2100. SSP2–4.5 is a “middle-of-the-road” scenario, with moderate policy interventions, emissions stabilization by mid-century, and warming of about 2.7 °C. SSP3–7.0 reflects a fragmented world with weak international coordination, high emissions, and projected warming of approximately 3.6 °C. SSP5–8.5 illustrates a fossil fuel driven development pathway with rapid economic growth and heavy reliance on carbon-intensive technologies, resulting in warming of around 4.4 °C.

The climate data used in the GAEZ model include monthly averages of maximum and minimum temperature, precipitation, relative humidity, wind speed, and shortwave radiation. These were derived from bias-corrected projections of the CAS-ESM2 Earth System Model under the ScenarioMIP framework (Dong et al., 2021). In addition to climate inputs, the GAEZ model incorporates biophysical constraints including soil, topography, and land use. Soil data were obtained from the Harmonized World Soil Database (Wieder et al., 2014), covering properties such as texture class, organic carbon content, pH, base saturation, and effective rooting depth. Topographic information was sourced from the Shuttle Radar Topography Mission (SRTM). To ensure consistency in land availability under future scenarios, we incorporated simulated land use projections generated by the GM-FLUS model. For further technical details on the structure and calibration of the GM-FLUS and GAEZ

models, see Jiang et al.(2020) and Li et al.(2023).

To enhance the accuracy and cross-scenario consistency of the 2030 rice yield projections, we applied a province-level normalization based on the relationship between GAEZ-simulated and officially reported yields in the baseline year 2020 (NBSC, 2021b). Specifically, we derived a correction factor for each province from the ratio of its GAEZ-estimated yield to the corresponding officially reported yield in 2020. This factor was then applied to scale the raw 2030 GAEZ projections, ensuring that interprovincial yield differentials align with observed productivity levels. The adjusted projected yield for province j in 2030, denoted as $\hat{Y}_{2030,j}$, is computed as:

$$\hat{Y}_{2030,j} = \left(\frac{Y_{2020,j}^{OBS}}{Y_{2020,j}^{GAEZ}} \right) \cdot Y_{2030,j}^{GAEZ} \quad (5)$$

where $Y_{2020,j}^{GAEZ}$ is the GAEZ-estimated yield in 2020; $Y_{2020,j}^{OBS}$ is the corresponding officially reported yield from official statistics (NBSC, 2021b), and $Y_{2030,j}^{GAEZ}$ is the unadjusted GAEZ-projected yield for 2030 under a given climate scenario.

2.3. Optimizing interprovincial rice distribution to achieve low-carbon goals

To explore feasible low-carbon strategies for China's future rice distribution, we develop a linear programming optimization framework that minimizes total greenhouse gas (GHG) emissions embedded in the interprovincial rice supply network. The objective function captures both production-related emissions—based on the carbon intensity of rice produced in each province—and transport-related emissions—derived from interprovincial trade distances. To enhance realism and policy relevance, the model incorporates several key constraints. First, it uses projected provincial-level rice production under four Shared Socioeconomic Pathways (SSPs: SSP1–2.6, SSP2–4.5, SSP3–7.0, and SSP5–8.5), integrating climate-adjusted yield potential from the GAEZ model and land-use changes from the GM-FLUS model. Second, it accounts for future rice consumption demand, which reflects expected demographic shifts and a gradual decline in per capita rice intake. Third, it applies interprovincial transport distance constraints to restrict implausible flows and reflect basic logistical feasibility. This framework is applied to both the baseline year (2020) and the future year (2030), enabling a dynamic comparison of current and optimized rice trade structures.

The objective is to minimize the total carbon footprint of rice consumption across all provinces as follows:

$$\min \sum_i \sum_j T_{ij} \cdot CF_{ij} \quad (6)$$

where T_{ij} is the quantity of rice transported from province j to province i (in tons), and CF_{ij} represents the total carbon footprint per ton of rice transported from j to i (kg CO₂-eq/ton), including both production and transport emissions. CF_{ij} is computed as:

$$CF_{ij} = EF_j + TC_{ij} \quad (7)$$

where EF_j denotes the emission factor for rice production in province j in kg CO₂-eq/ton (refer to Eq. (4)), and TC_{ij} is the transport-related emission from province j to province i in kg CO₂-eq/ton, calculated as:

$$TC_{ij} = Dist_{ij} \cdot EF_{trans} \quad (8)$$

where EF_{trans} represents the standardized emission factor per tonne-kilometre for rail transport, as reported in the UK Government's Greenhouse Gas Reporting(UK, 2023), and $Dist_{ij}$ represents transport distance from province j to province i , based on the measurements in Gao et al. (2014).

The optimization is subject to the following constraints:

Demand constraint: The total amount of rice inflow into province i from all supplying provinces must equal the rice demand of province i .

$$\sum_j T_{ij} = D_i \quad (9)$$

Supply constraint: The total quantity of rice distributed from province j to all receiving provinces must not exceed the total rice production of province j . This constraint assumes that all provincial production is potentially available for distribution under normal conditions, excluding government-held strategic reserves, which are typically mobilized only under emergency scenarios and for which detailed data are not publicly accessible.

$$\sum_i T_{ij} \leq Y_j \quad (10)$$

Non-negativity constraint: Trade volumes must be non-negative:

$$T_{ij} \geq 0 \quad (11)$$

The optimization problem is formulated as a linear programming (LP) model and solved using the lpSolve package in R. For each SSP scenario in 2030, the model generates an optimal rice flow matrix that minimizes national consumption-based carbon emissions, subject to provincial supply and demand constraints. Future rice production levels are derived from the adjusted yield projections produced by the GAEZ model under each SSP scenario. Provincial rice consumption in 2030 is estimated by extrapolating 2020 baseline values in line with recent national dietary trends. Empirical evidence indicates that per capita rice consumption has stabilized in urban areas but continues to decline among rural populations. Based on projections by Chen et al.(2020), rural per capita rice consumption is expected to decline to approximately 88 % of its 2020 level by 2030. This adjustment is incorporated into the model's province-level demand forecasts.

3. Results

3.1. Spatial patterns of interprovincial rice trade in China

The observed interprovincial rice trade in China for the baseline year 2020 is presented in Fig. 2. The spatial distribution reveals significant regional disparities in rice supply and demand across provinces. Major rice-producing provinces, notably Heilongjiang (HLJ), Jilin (JL), Hubei (HUB), and Jiangxi (JX), collectively accounted for approximately 63 % of total rice exports, forming critical supply hubs within the national rice trade network. Key rice-importing provinces included Guangdong (GD), Hebei, Shandong, and Zhejiang (ZJ), which together received approximately 67 % of the total interprovincial rice inflow. Interestingly, several provinces exhibited pronounced long-distance trade patterns, such as the substantial rice flows from HLJ to Guangdong, ZJ, and Shanghai (SH). This highlights that distance and transportation cost may not be the dominant factor shaping rice circulation patterns in China. Additionally, provinces located in Central China, including HUB and Anhui (AH), showed balanced trade profiles with moderate export and import flows, suggesting a relatively stable intra-regional rice distribution system. Several western provinces exhibited limited participation in the rice trade network, indicating a relatively high degree of self-sufficiency or reliance on alternative food sources. Using province-specific emission factors, we also estimated the carbon embedded in traded rice volumes (Figure S3), thereby tracing the transfer of production-side emissions to consumption destinations.

3.2. Projected provincial rice production in 2030 under future climate scenarios

Fig. 3 presents projected provincial rice production in China for 2030 under four representative climate and socio-economic scenarios (SSP1–2.6, SSP2–4.5, SSP3–7.0, and SSP5–8.5). The simulations reveal

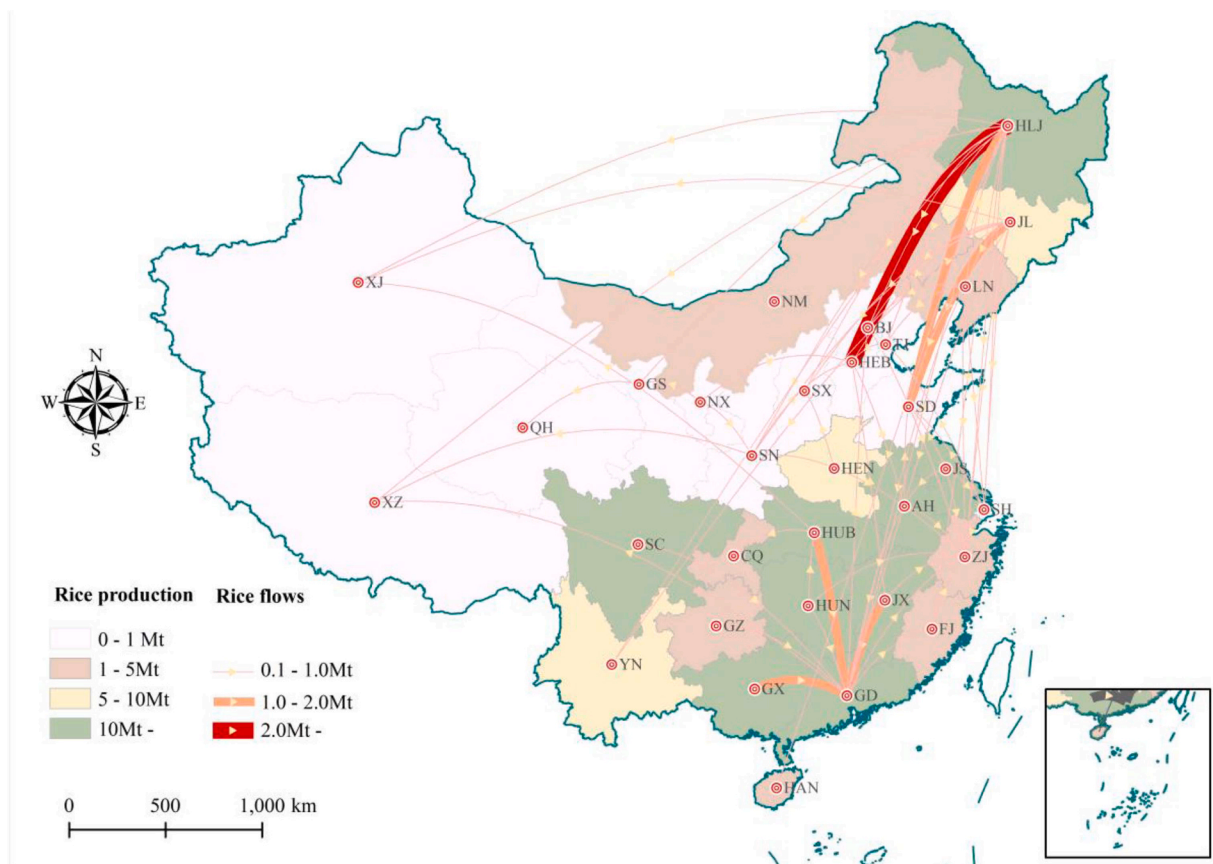


Fig. 2. Interprovincial rice trade flows in China, 2020. Note: The fill color of each province represents its total rice production in 2020. Arrows indicate interprovincial rice trade flows, with arrow widths proportional to trade volumes. Arrow directions reflect the flow of rice from production to consumption provinces. Trade data are based on observed sample records.

pronounced spatial disparities in production potential across all scenarios. Provinces such as Hunan (HUN), Heilongjiang (HLJ), Jiangxi (JX), and Hubei (HUB) consistently emerge as leading producers, each projected to exceed 20 million tons (Mt). These provinces demonstrate relatively high production resilience, though moderate fluctuations are observed in response to changes in climate and land use. By contrast, the middle and lower Yangtze River basin, the eastern Sichuan Basin, and South China are projected to experience significant production declines—particularly under SSP2–4.5 and SSP5–8.5 (see Figure S4). Conversely, a few provinces show stable or slightly increased yields under low-emission scenarios, suggesting that sustainable development pathways may partially offset climate-induced productivity losses. Overall, the results point to a continued geographic concentration of rice production in traditional regions, highlighting the critical need for targeted adaptation strategies and greater attention to regional disparities in future food security planning.

3.3. Optimized interprovincial rice trade patterns under four climate scenarios

Fig. 4 presents spatially explicit maps of the optimized interprovincial rice trade networks in 2030 under four climate scenarios, each calibrated to minimize consumer-side carbon footprints. Compared to the baseline configuration in 2020, the optimized flows exhibit notable spatial reconfigurations driven by shifts in regional production capacity. Under SSP5–8.5, for instance, northern provinces such as Heilongjiang (HLJ) and Jilin (JL) expand their outbound rice flows, reflecting projected production gains under high-emission climate conditions. In contrast, traditional suppliers like Hunan (HUN) and Jiangxi (JX), which have higher per-ton emission intensities, play a diminished role in the

optimized trade structure. Together, these scenario-specific patterns demonstrate the adaptability of China’s rice distribution system and highlight the importance of forward-looking, regionally tailored strategies to promote climate-resilient and low-carbon food supply chains.

3.4. Net embedded carbon flows by province across scenarios

Fig. 5 illustrates net embedded carbon flows by province under the optimized interprovincial rice distribution for the baseline year 2020 and for 2030 across four climate scenarios (SSP1–2.6, SSP2–4.5, SSP3–7.0, SSP5–8.5). The results reveal substantial spatial and temporal variation in carbon flow roles. Provinces such as Guangdong (GD) and Zhejiang (ZJ) consistently appear as net importers of embedded carbon, with varying levels of dependency across scenarios. In contrast, traditional rice producers—including Heilongjiang (HLJ), Jilin (JL), and Jiangsu (JS)—remain primary net exporters, although the magnitude of their carbon outflows shifts in response to changes in emission intensity and production levels. These patterns underscore the dynamic redistribution of carbon responsibilities under climate change and highlight the need for flexible, region-specific strategies to support low-carbon rice supply chains.

3.5. National carbon emissions from interprovincial rice distribution: baseline vs optimized scenarios

Table 1 summarizes national-level carbon emissions from interprovincial rice distribution under both observed and optimized trade scenarios. In the baseline year 2020, actual trade flows generated 60.01 Mt CO₂eq of embedded emissions. When reconfigured to minimize consumer-side carbon footprints under the same supply and demand

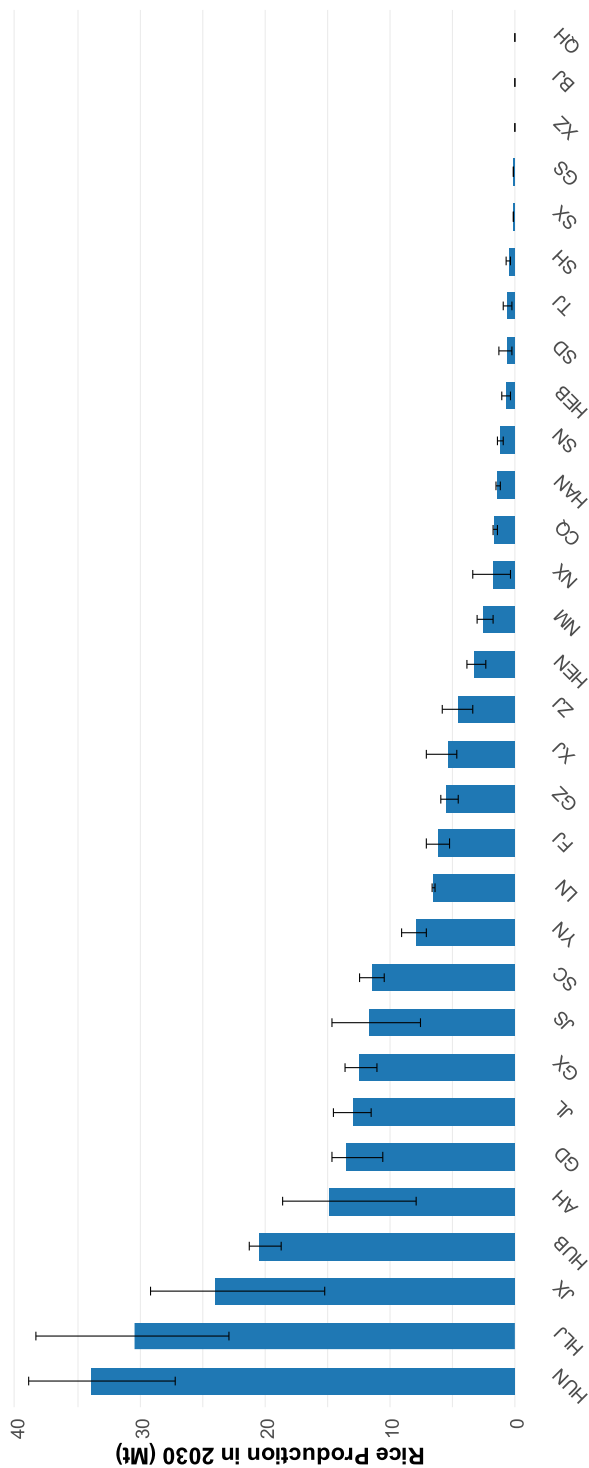


Fig. 3. Projected provincial-level rice production in China for 2030 under four climate and socio-economic scenarios (SSP1–2.6, SSP2–4.5, SSP3–7.0, and SSP5–8.5). Note: Production estimates were simulated using the Global Agro-Ecological Zones (GAEZ) and GM-FLUS models, incorporating scenario-specific changes in climate conditions, land-use patterns, and crop suitability. The vertical error bars represent the range of simulated rice yields for each province across the four scenarios, reflecting uncertainties arising from differences in future climate trajectories and land-use dynamics.

constraints, emissions drop to 50.36 Mt CO₂eq, representing a 16.1 % reduction (Figure S6). Looking ahead to 2030, the model projects that optimized rice distribution under all four Shared Socioeconomic Pathway (SSP) climate scenarios would further lower emissions to between 47.69 and 48.36 Mt CO₂eq. These reductions represent an emission abatement of 19.4 % to 20.5 % relative to the 2020 baseline. These findings underscore the significant carbon mitigation potential of strategic, emissions-aware reallocation of interprovincial rice flows. Regardless of future climate trajectories, reconfiguring rice trade networks offers a robust and scalable pathway toward low-carbon transitions in China’s agri-food system.

4. Discussion

This study offers novel empirical insights into China’s interprovincial rice distribution system and the associated carbon emissions embedded in food trade under both current and future conditions. Contrary to the widely held assumption that trade follows a distance-minimizing logic, our analysis reveals extensive long-distance rice flows shaped by complex socio-economic, institutional, and infrastructural factors, rather than by transportation costs alone. The observed distribution network reveals significant transfers of carbon emissions from major rice-producing provinces to distant consumption hubs, underscoring substantial spatial heterogeneity in carbon accountability. Looking ahead, integrated land-use and climate projections suggest major regional shifts in rice production capacity by 2030, reshaping national supply dynamics. Under future climatic conditions, optimization modeling demonstrates that a consumption-oriented reallocation of rice flows could reduce total embedded carbon emissions by up to 20.5 percent relative to baseline levels. These findings underscore the importance of incorporating spatially explicit production shifts and carbon intensities into food system planning to support climate-resilient and low-carbon transitions.

By drawing on observed interprovincial rice trade data (Fig. 2), this study addresses key limitations of conventional simulation-based approaches, which typically rely on stylized production-consumption balancing and assume cost-minimizing shortest-path routing. Such models often neglect the influence of policy incentives, logistical infrastructure, and institutional factors, thereby risking misrepresentation of actual trade patterns and their environmental outcomes. In contrast, our analysis reveals substantial long-distance rice transfers. For instance, flows from Heilongjiang (HLJ) to Guangdong (GD) and from Jilin (JL) to Shandong (SD) deviate significantly from predictions based solely on transport cost minimization (see Figure S5). These discrepancies suggest that distance-based assumptions are less relevant in modern China, where logistical advancements have significantly lowered the marginal costs of long-haul grain transport. By incorporating province-specific consumption structures and observed trade behaviors, our approach offers a more realistic and policy-relevant representation of rice circulation and its associated carbon footprint, aligning better with on-the-ground dynamics than traditional simulation models.

The projected spatial disparities in rice production capacity by 2030 reflect heterogeneous regional responses to climate change and land-use transitions (Fig. 3), carrying significant implications for national food security. Unlike previous studies, which often assessed rice yields solely based on climatic variables, our analysis integrates both dynamic agroclimatic conditions and evolving cropland patterns, offering a more realistic representation of future agricultural systems. To validate our projections, we conducted separate validation exercises for the land-use and rice-yield simulations. The land-use validation yielded a Kappa coefficient of 0.65 when comparing the simulated 2020 results against remote-sensing observations, indicating moderate-to-high agreement. For rice-yield validation, we simulated production for 2020 using actual climate, land-use, and cultivated area data in the GAEZ model. The estimated national yield was approximately 268.65 million tons—roughly 1.27 times the reported value. This discrepancy is expected,

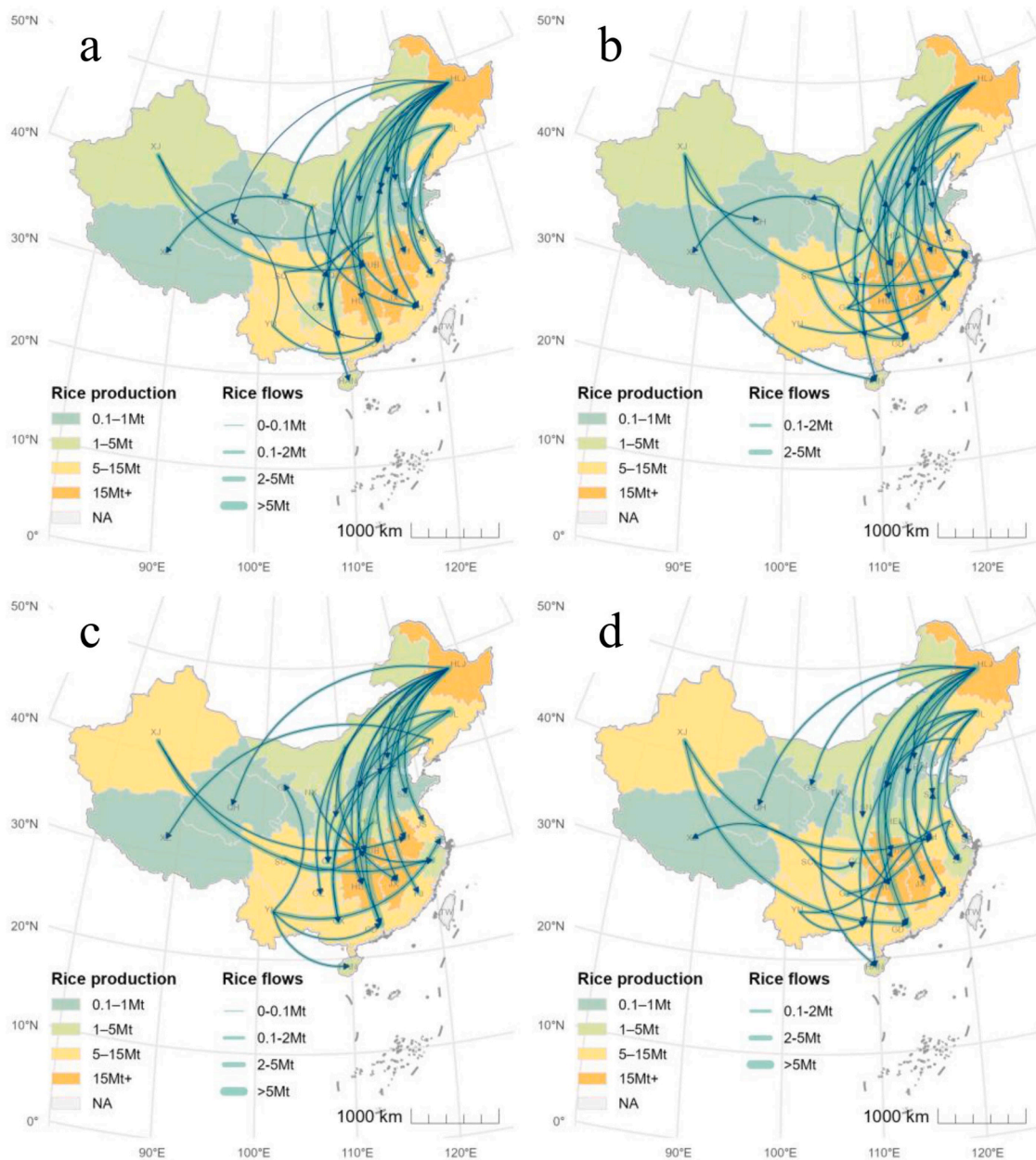


Fig. 4. Optimized interprovincial rice trade patterns under four climate scenarios (SSP1–2.6, SSP2–4.5, SSP3–7.0, and SSP5–8.5) projected for 2030. Note: Panels (a)–(d) depict the optimized rice trade flows that minimize consumption-based carbon footprints under SSP1–2.6, SSP2–4.5, SSP3–7.0, and SSP5–8.5, respectively. Arrow widths represent trade volumes (Mt), with direction indicating flows from production to consumption provinces. Scenario-specific differences highlight spatial shifts in rice production and the resulting adaptations in low-carbon distribution strategies.

as the GAEZ model estimates agroecologically attainable potential rather than actual observed yields. At the provincial scale, simulated yields showed strong agreement with reported data (Pearson correlation coefficient = 0.82), aligning closely with prior validation studies (e.g., Liu et al., 2014). These validation results reinforce the robustness of our projections and their relevance for policy decision-making.

By optimizing future rice distribution networks, this study identifies a viable pathway toward a low-carbon transformation in response to climate change. Optimization scenarios aimed at minimizing consumption-based carbon emissions reveal significant departures from historical trade patterns (Fig. 4). Southern provinces, such as Hunan and Jiangxi, traditionally major rice exporters, are projected to have reduced roles in future distribution due to their relatively high per-ton emission intensities. In contrast, northern provinces, notably Heilongjiang and Jilin, are anticipated to become strategically more important, benefiting

from enhanced agroecological suitability and rising yield potentials under changing climatic conditions. These projected shifts suggest that China’s future rice distribution landscape will increasingly rely on low-carbon, climate-resilient production zones. This emphasizes the need for adaptive and forward-looking infrastructure investments and policy frameworks to ensure an equitable and sustainable transition of the food system.

This study has several limitations that merit further exploration. First, the model does not incorporate government-held strategic rice reserves, which are typically reserved for emergency use rather than routine distribution. Given our focus on optimizing regular supply flows under standard market conditions, this exclusion is unlikely to bias the results. Second, while we focus on CH₄ and N₂O, the two dominant greenhouse gases in rice cultivation, this targeted approach may slightly underestimate the total carbon footprint. Nevertheless, CH₄ and N₂O

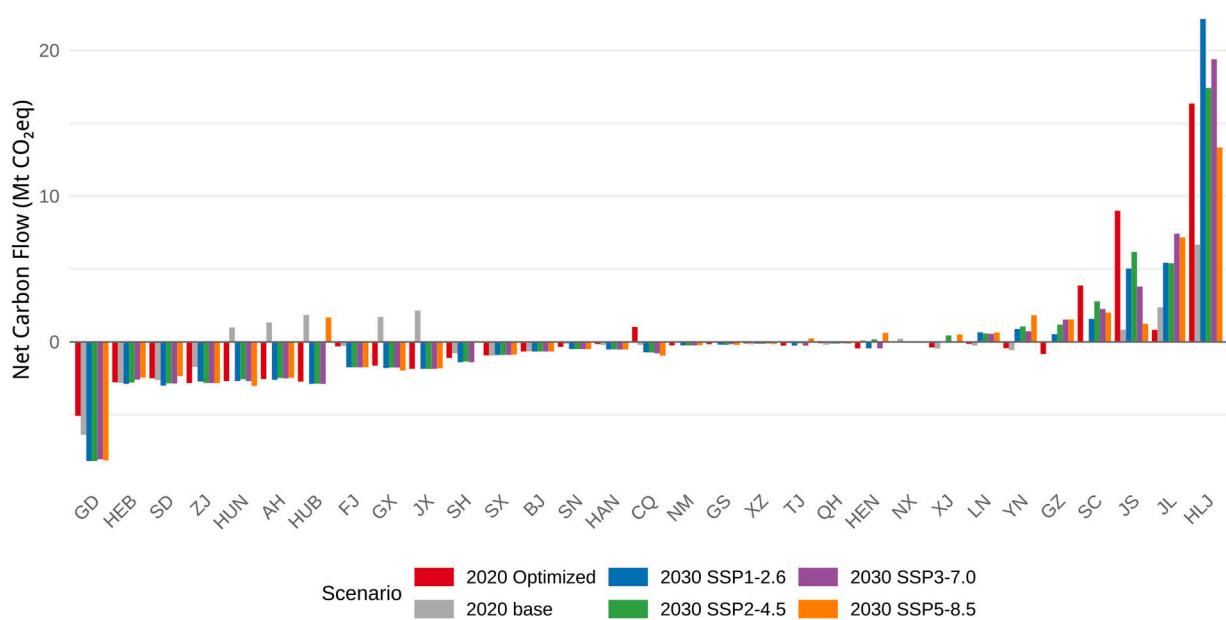


Fig. 5. Net embedded carbon flows under optimized interprovincial rice distributions: 2020 Baseline vs 2030 projections across four climate scenarios. Note: Positive values indicate provinces that are net exporters of embedded carbon (net exporter), while negative values indicate net importers (net consumers).

Table 1

National total carbon emissions from interprovincial rice trade under baseline, optimization, and climate scenario projections.

Scenario Description	Carbon Emissions (Mt CO ₂ eq)	Reduction Rate
Baseline (2020)	60.01	-
Optimized (2020)	50.36	16.1 %
SSP1-2.6 (2030)	48.36	19.4 %
SSP2-4.5 (2030)	48.02	20.0 %
SSP3-7.0 (2030)	47.69	20.5 %
SSP5-8.5 (2030)	48.23	19.6 %

account for most emissions and exhibit substantial interprovincial variation, making them highly relevant for identifying effective and region-specific mitigation strategies. Finally, although the model incorporates key projected changes in future supply, demand, and transportation costs, we recognize that rice trade patterns may also be influenced by additional dynamic factors, such as price volatility and policy interventions. Incorporating these dimensions in future research would help to further improve the model’s comprehensiveness and practical relevance.

5. Policy implications

Our findings highlight the importance of aligning rice production and distribution systems with both climate adaptation and carbon mitigation goals. The spatial redistribution of embedded carbon emissions through interprovincial rice trade reveals critical entry points for integrated policy design.

First, our projections suggest a spatial shift in rice production potential under climate and land-use changes (Fig. 3). Integrating such future dynamics into national food security planning is crucial. Strategic support should be directed to provinces projected to gain comparative advantages in production, including expanded insurance coverage, climate-smart extension services, and incentives for low-emission technologies.

Second, our analysis shows that current rice distribution patterns involve extensive long-distance transfers (Fig. 4), such as those from Heilongjiang to Guangdong, which deviate from simple cost-minimization assumptions. This suggests a need to incorporate

empirical trade behaviors and regional consumption preferences into agricultural logistics and infrastructure planning. Policymakers should invest in upgrading interprovincial transport and storage systems based on observed trade flows, rather than relying solely on theoretical distances.

Third, the optimization scenarios demonstrate that aligning rice distribution with regional agroecological advantages, particularly by leveraging low-emission, high-yield provinces such as Heilongjiang and Jilin—can reduce embedded carbon emissions by up to 20.5 % by 2030 (Table 1). To support this transition, targeted fiscal and infrastructure support is essential. These include low-interest agricultural credit, tailored subsidies for low-emission producers, and investments in modern grain storage and transport facilities to strengthen supply chain resilience.

6. Conclusion

This study integrates empirically observed interprovincial rice trade data, scenario-based projections of land use and climate change, and carbon-focused optimization modeling to characterize the spatial patterns and future trajectories of emissions embedded in China’s rice distribution network. Our results show that current trade flows drive substantial transfers of production-side emissions to major consumption centers, with pronounced spatial heterogeneity in provincial carbon responsibilities. Scenario-driven optimization targeting consumer-side emissions demonstrates considerable mitigation potential, reducing national emissions by up to 20.5 % relative to the baseline. By 2030, shifts in climate and land use are projected to reshape the geography of rice production and consumption, reconfiguring carbon flows across provinces. By combining empirical flows, forward-looking scenarios, and optimization strategies, this study addresses key knowledge gaps and provides robust evidence to inform low-carbon transitions in food supply chains. The findings underscore the need for regionally differentiated policy measures and interprovincial coordination to reduce emissions. Future work should build on this framework to support integrated planning of food production and distribution systems, enabling source-level mitigation and accelerating the sustainable transformation of China’s agri-food sector.

- groundwater depletion and environmental footprints without compromising production. *Commun. Earth. Environ.* 5, 380. <https://doi.org/10.1038/s43247-024-01547-9>.
- Sun, J., Sun, S., Yin, Y., Wang, Y., Zhao, J., Tang, Y., Wu, P., 2023. Water-carbon" redistribution caused by China's interprovincial grain transportation. *Water Res.* 235, 119894. <https://doi.org/10.1016/j.watres.2023.119894>.
- UK, 2023. Greenhouse Gas reporting: Conversion Factors 2023 – Condensed Set. UK Department for Energy Security and Net Zero. Version 1.0. Available at <https://www.gov.uk/government/publications/greenhouse-gas-reporting-conversion-factors-2023>. UK Government.
- United States Environmental Protection Agency, 2023. Climate change impacts on agriculture and food supply.
- Wieder, W.R., Boehnert, J., Bonan, G.B., Langseth, M., 2014. Regridded Harmonized World Soil Database 1, 2. <https://doi.org/10.3334/ORNLDAAAC/1247>.
- Winkler, K., Fuchs, R., Rounsevell, M., Herold, M., 2021. Global land use changes are four times greater than previously estimated. *Nat. Commun.* 12, 2501. <https://doi.org/10.1038/s41467-021-22702-2>.
- Wu, S., Ben, P., Chen, D., Chen, J., Tong, G., Yuan, Y., Xu, B., 2018. Virtual land, water, and carbon flow in the inter-province trade of staple crops in China. *Resour. Conserv. Recycl.* 136, 179–186. <https://doi.org/10.1016/j.resconrec.2018.02.029>.
- Xuan, X., Zhang, F., Deng, X., Bai, Y., 2023. Measurement and spatio-temporal transfer of greenhouse gas emissions from agricultural sources in China: a food trade perspective. *Resour. Conserv. Recycl.* 197, 107100. <https://doi.org/10.1016/j.resconrec.2023.107100>.
- Yang, Dajin, Li, Ning, 2014. *Handbook On National Food Pollution and Hazardous Factors*.
- Yang, J., Gao, B., Xia, F., Wei, H., Fan, S., 2025. Internalizing the external costs to achieve environmental and economic goals: A case study of rice production in China. *Food Policy* 132, 102857. <https://doi.org/10.1016/j.foodpol.2025.102857>.
- Yang, J., Wang, J., Xu, C., Liu, Y., Yin, Q., Wang, X., Wang, L., Wu, Y., Xiao, G., 2021. Rice supply flows and their determinants in China. *Resour. Conserv. Recycl.* 174, 105812. <https://doi.org/10.1016/j.resconrec.2021.105812>.
- Yue, Y., Yang, W., Wang, L., 2022. Assessment of drought risk for winter wheat on the Huanghuaihai Plain under climate change using an EPIC model-based approach. *Int. J. Digit. Earth.* 15, 690–711.
- Zhang, L., Yang, Z., Nan, Q., Cheng, Y., Li, H., 2023. Evaluation method and empirical study of greenhouse gas emissions from a city-scale rice field system based on LCA: taking Taizhou City as an example. *J. Earth Environ.* 796–808.
- Zhao, L., He, Y., 2018. *China Residents Nutrition and Health Status Monitoring Report*. People's Medical Publishing House, Beijing.
- Zuo, C., Wen, C., Clarke, G., Turner, A., Ke, X., You, L., Tang, L., 2023. Cropland displacement contributed 60% of the increase in carbon emissions of grain transport in China over 1990–2015. *Nat. Food* 4, 223–235. <https://doi.org/10.1038/s43016-023-00708-x>.